Available online at www.sciencedirect.com
SCIENCE DIRECT®
Journal of Power Sources 134 (2004) 7–17
JOURNAL OF POWER SOURCES
www.elsevier.com/locate/jpowsour

Preparation, electrical, mechanical and thermal properties of composite bipolar plate for a fuel cell

Hsu-Chiang Kuan [a], Chen-Chi M. Ma [a,*], Ke Hong Chen [a], Shih-Ming Chen [b]

[a] *Department of Chemical Engineering, National Tsing-Hua University, Hsin-Chu 30043, Taiwan, ROC*
[b] *Materials Research Laboratories, Industrial Technology Research Institute, Hsin-Chu, Taiwan, ROC*

Received 23 December 2003; accepted 24 February 2004

Available online 25 May 2004

Abstract

A novel composite bipolar plate for a polymer electrolyte fuel cell has been prepared by a bulk-moulding compound (BMC) process. The electrical resistance of the composite material decreases from 20 000 to 5.8 mΩ as the graphite content is increased from 60 to 80 wt.%. Meanwhile, the electrical resistance of composite increases from 6.5 to 25.2 mΩ as the graphite size is decreased from 1000 to 177 μm to less than 53 μm. The thermal decomposition of 5% weight loss of composite bipolar plate is higher than 250 °C. The oxygen permeability of the composite bipolar plate is 5.82×10^{-8} (cm^3/cm^2 s) when the graphite content is 75 wt.%, and increases from 6.76×10^{-8} to 3.28×10^{-5} (cm^3/cm^2 s) as the graphite size is longer or smaller than 75 wt.%. The flexibility of the plate decreases with increasing graphite content. The flexural strength of the plate decreases with decrease in graphite size from 31.25 MPa (1000–177 μm) to 15.96 MPa (53 μm). The flexural modulus decreases with decrease of graphite size from 6923 MPa (1000–177 μm) to 4585 MPa (53 μm). The corrosion currents for plates containing different graphite contents and graphite sizes are all less than 10^{-7} A cm^{-2}. The composite bipolar plates with different graphite contents and graphite sizes meet UL-94V-0 tests, and the limiting oxygen contents are higher than 50. Testing show that composite bipolar plates with optimum composition are very similar to that of the graphite bipolar plate.

Keywords: Fuel cell; Bipolar plate; Polymer composite; Bulk-moulding compound

1. Introduction

Polymer electrolyte membrane fuel cells (PEMFCs) are most promising power sources for road transportation and portable applications. With the bipolar plate accounting for the bulk of the stack, it is desirable to fabricate plates that are as thin and lightweight as possible. Bipolar plates electrically connects successive cells in a fuel-cell stack, and also provide the gas supply. Hence, bipolar-plate materials have to be inexpensive, easy to machine or shape and lightweight. They must also possess good mechanical properties and thermal stability, with low contact resistance. Traditionally, the most commonly used bipolar plate material is graphite. Among the advantages of graphite are excellent resistance to corrosion and low bulk resistivity. On the other hand, the disadvantages are its cost, the difficulty in machining, and its brittleness [1–3]. Because of the brittleness of graphite, the bipolar plate requires a thickness of the order of several millimeters, and this causes the fuel-cell stack to be heavy and voluminous [4]. Metal is also a good material for a bipolar plate, it offers the attributes of good electrical conductivity, low cost, excellent mechanical properties, and ease of fabricate. Metal is, however, unable to resist corrosion in fuel cells [5–8]. A composite bipolar plate is a promising alternative to graphite, and has the advantages of low cost, ease in machining, good corrosion resistance and low weight [9,10].

A composite bipolar plate containing vinyl ester and graphite powder can be prepared by a bulk-moulding compound (BMC) process. The graphite content used in preparing composite bipolar plates is extremely important in determining the resultant electrical conductivity and mechanical properties [4]. A high graphite content will enhance the electrical conductivity of the composite bipolar plate, but will make the BMC process more difficult. This study examines the effect of graphite content and size of graphite powder on the electrical, physical, mechanical and thermal properties of a composite bipolar fuel cell. A comparison is also made of the current–voltage performance of composite and graphite bipolar plates.

* Corresponding author. Fax: +886-3571-5408.
E-mail address: ccma@che.nthu.edu.tw (C.-C.M. Ma).

0378-7753/$ – see front matter © 2004 Elsevier B.V. All rights reserved.
doi:10.1016/j.jpowsour.2004.02.024

Table 1
Formulation of BMC process

Component	Composition	
	Resin composition	BMC composition
Vinyl ester[a] (wt.%)	75	20–40
Low profile agent (wt.%)	8	
Styrene monomer (wt.%)	17	
TBPB (phr)[b]	l.8	
Zinc stearate (phr)	3.5	
Magnesium oxide (phr)	1.8	
Graphite powder (wt.%)		60–80
Total (wt.%)		100

[a] Chemical structure of phenolic-novolac, epoxy-based, vinyl ester resin is as follows:

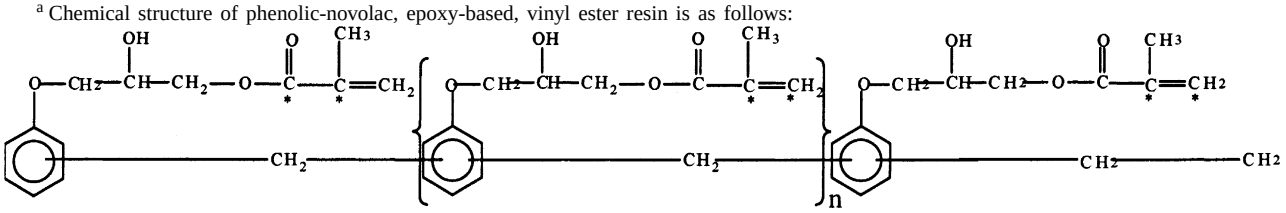

[b] phr: parts per hundred parts of resin, based on amount of vinyl ester + low profile agent + styrene monomer.

2. Experimental

2.1. Materials

Phenolic-novolac, epoxy-based, vinyl ester resin was used (as shown in Table 1), which was provided by the Swancor Industrial Corporation, Taiwan. Graphite powder was obtained from Great Carbon Co. Ltd., Taiwan. The density of the power was 1.88 and the particle size is smaller than 1000 μm. Various sizes of graphite particle (1000–177, 177–125, 125–74, 74–53 μm, less than 53 μm) were also prepared by the screen mesh method.

2.2. Preparation of BMC material

Preparation of the resin involved mixing together vinyl ester, low profile agent (PS/SM series), styrene monomer, thickening agent (MgO) and release agent (ZnSt). The BMC formulation is given in Table 1. The BMC material was prepared by compounding resin and graphite in a kneader for 30 min. The BMC was thickened for 48 h. before the hot-pressing process. The processing temperature was 140 °C and the processing time was 5 min.

2.3. Density analysis

The density of each sample was measured according to the ASTM D792 test procedure. The specimen was weighed in air and the value was recorded as A. The specimen was completely immersed in water at 23 ± 2 °C. The suspended specimen was weighed and recorded as B. The density of the sample was defined as $A/(A - B)$.

2.4. Porosity analysis

The porosity of each sample was determined according to the ASTM C20 test procedure. The specimen was weighed in air and the value was recorded as D. The specimen was then completely immersed in water at a temperature of 100 °C for 2 h and cooled in water for 12 h. The specimen was weighed and recorded as S. The specimen was then dried and weighed, S_w. The porosity was calculated as follows:

$$B_s \text{ (buoyancy of specimen)} = W \text{ (specimen weight in air)} - S \text{ (suspened specimen weight)} \quad (1)$$

$$B_s \text{ (buoyancy of specimen)} = d \text{ (density of water)} \times V \text{ (specimen volume)} \quad (2)$$

$$V \text{ (specimen volume)} = W \text{ (specimen weight in air)} - S \text{ (suspended specimen weight)} \quad (3)$$

$$S_w \text{ (saturated weight)} - D \text{ (specimen dry weight)} = d \text{ (density of water)} \times V'' \text{ (specimen void volume)} \quad (4)$$

$$V'' \text{ (specimen void volume)} = S_w - D \quad (5)$$

$$\text{Porosity (\%)} = \frac{V''}{V} \times 100$$

2.5. Optical microscopy

The morphology and number of the voids in the composite bipolar plate were examined by means of an optical microscope (BH, Olympus, Japan).

2.6. Electrical resistance analysis

The electrical resistance of the composite bipolar plate was examined with a four point probe detector (C4S-54/5S, Cascade Microtech, USA).

2.7. Thermomechanical analysis (TMA)

The TMA test was performed according to the procedure of ASTM E831. The glassy transition temperature (T_g) of vinyl ester and the thermal expansion were measured by TMA (TMA2940, DUPont, USA) from room temperature to 250 °C with a heating rate of 10 °C/min under a nitrogen atmosphere. The measurements were conducted using a 1 mm^2 sample. Plots of dimension changes versus temperature were recorded.

2.8. Thermogravimetric analysis (TGA)

Thermal degradation of vinyl ester was measured by TGA (TA2000, DUPont, USA) from room temperature to 800 °C with a heating rate of 10 °C/min under a nitrogen atmosphere. The measurements were conducted using 6–10 mg samples. Plots of weight loss versus temperature were recorded.

2.9. Oxygen permeability analysis

The oxygen permeability of the composite bipolar plate was examined by means of a gas permeability tester (APP2100, Porous Materials Inc., USA).

2.10. Flexural strength and flexural modulus test

A universal testing machine (Instron Model 4468) was used to investigate the flexural property of the composite bipolar plate. The flexural strength and flexural modulus test were performed according to the procedure of ASTM D 790 with a specimen bar of 60 mm in length, 13 mm in width, and 3 mm in thickness. The supporting span is 60 mm and the rate of the crosshead was 1 mm/min.

2.11. Corrosion test

The corrosion resistance of the composite bipolar plate was examined with a potentiostat (potentialstat, Autolab, USA). Plots of voltage versus current were recorded. Tafel plots were used to determine the corrosion current.

2.12. Limiting oxygen index (LOI) test

The LOI is defined as the minimum fraction of O_2 in a mixture of O_2 and N_2 that will just support flaming combustion. The LOI test was performed according to the procedure of the ASTM D 2836 oxygen index method with a specimen bar of 7–15 cm in length, 6.5 ± 0.5 mm in width, and 3.0 ± 0.5 mm in thickness. A Bunsen burner was used to ignite the sample bars, which were suspended vertically. The flame was removed and the timer was started. The concentration of oxygen was raised if the specimen used burning before 3 min or 5 cm. The oxygen content was adjusted until the limiting concentration was determined.

2.13. UL-94 vertical test

The UL-94 vertical test was performed according to the procedure of ASTM D 3801. Five sample bars, suspended vertically over surgical cotton, were iginited by a Bunsen burner. A flame was applied twice to the lower end of the specimen for 10 s. The UL-94V-0 specification is achieved if each after-flame time does not exceed 10 s, and sum of the after-flame time for the five samples does not exceed 50 s. The surgical cotton below the specimen should not be ignited with flaming drippings.

2.14. I–V performance test

The membrane electrode assembly (MEA) was purchased from ElectroChem Co., USA. It was an FC50-MEA (Nafionll5), type with an active area of 25 cm^2. The dimensions of composite bipolar plate and graphite bipolar plate were both 10 cm × 10 cm × 3.5 cm. The twisting strength of the screw bolts was 40 kg cm. The performances of a single cell and a 6-cell stack were evaluated. The fuel was wet hydrogen gas (50 °C moisture) and dry oxygen gas. The flow rate of hydrogen/oxygen gas was 0.4/0.3 and 3/2 (L/min), respectively. When the cell temperature reached 50 °C, the current–voltage (*I–V*) curves were recorded.

3. Results and discussion

3.1. Density of composite

The density of the composite bipolar plate increases from 1.49 to 1.82 with increasing graphite content, see Fig. 1. The density of the composite decreases from 1.70 to 1.45 with the decreasing of graphite size, see Fig. 2. Increasing the graphite content will reduce the resin content. Since the density of vinyl ester resin (1.03) is much lower than that of

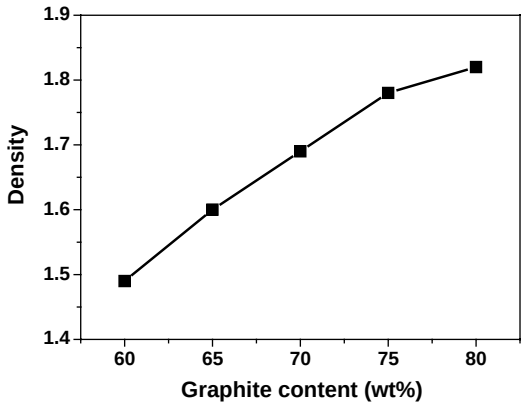

Fig. 1. Density of composite bipolar plate with different graphite contents.

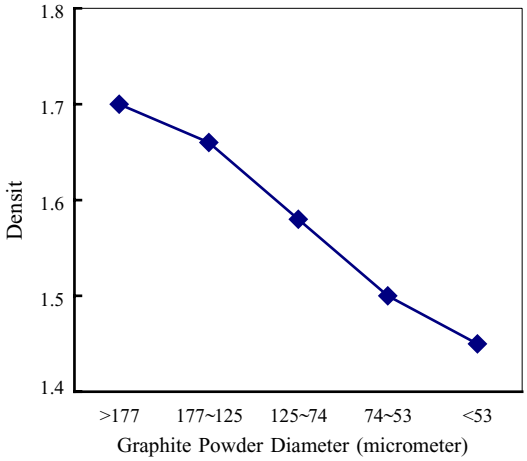

Fig. 2. Density of composite bipolar plate with 75 wt.% graphite content and with different graphite powder sizes.

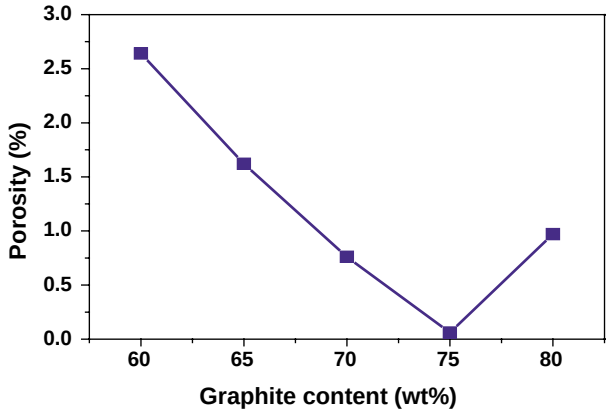

Fig. 3. Porosity of composite bipolar plate with different graphite contents.

graphite (1.88), the density of the composite bipolar plate increases with graphite content. Decreasing the graphite size will increase the voids in the composite bipolar plate. Consequently, density of the plate will be decreased. The density of the plate affects the weight of the fuel-cell stack. The maximum density of the plate for a composite with 80 wt.% graphite is 1.82, i.e., it is lower than that of a pure-graphite bipolar plate, viz. l.88.

3.2. Porosity of composite

The porosity of the composite bipolar plate reaches a minimum at 75 wt.% graphite content, see Fig. 3. The porosity increases with decrease in graphite size, i.e., from 0.57% (1000–177 μm) to 15.45% (less than 53 μm). The porosity may arise from evaporation of styrene monomer during the hot-pressing process. Furthermore, since graphite powder is not fully wetted by vinyl ester resin, insufficient vinyl ester resin may induce holes in the composite bipolar plate. The porosity of decreases with increase in graphite content to 75 wt.% to give a minimum value of 0.06%, and then increases as more graphite is added. The prosity increases as

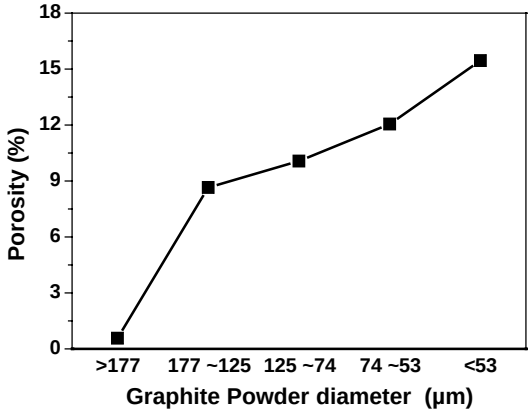

Fig. 4. Porosity of composite bipolar plate with 75 wt.% graphite content and with different graphite powder sizes.

the graphite size is decrease from 0.57% (1000–177 μm) to 15.45% (less than 53 μm), which is shown in Fig. 4.

3.3. Morphology

The morphology of composite bipolar plate with a graphite size of 1000–177 μm or less than 53 μm is shown in Figs. 5–10. Voids in the plate are clearly visible. The formation of voids is due to evaporation of styrene monomer and unwetted graphite powder. The number of voids is at a minimum at a graphite content of 75 wt.%, and is smaller for a graphite size of 1000–177 μm than for a size less than 53 μm.

3.4. Electrical properties

The electrical resistance of the composite bipolar plate decreases with increasing graphite content, i.e., from 2000 mΩ (60 wt.%) to 5.8 mΩ (80 wt.%). The electrical resistance increases with decreasing graphite size, i.e., from 6.5 mΩ (1000–177 μm) to 25.2 mΩ (less than 53 μm). The electrical resistance changes from 20 000 to 50 mΩ when the graphite content is increased from 60 to 65 wt.%. Insufficient graphite powder presents the formation of a electrical conductive matrix, and therefore, generates a huge electrical resistance between 60 and 65 wt.%. The electrical conductive matrix is formed when the graphite content is greater than 65 wt.%. There is only a slight decrease in electrical resistance between 65 and 80 wt.%. For example, the difference in electrical resistance is 1950 mΩ between 60 and 65 wt.%, but only 3.7 mΩ between 75 and 80 wt.%. Fig. 11 shows that addition of graphite powder to reduce the electrical resistance of the composite bipolar plate is not effective when the graphite content is over 75 wt.%.

The electrical resistance of the composite bipolar plate increases with decrease in graphite size as shown in Fig. 12. The conduction of electrons through graphite powder is enhanced if the powder is compacted. Aggregation of the powder increases as the particle size of graphite powder

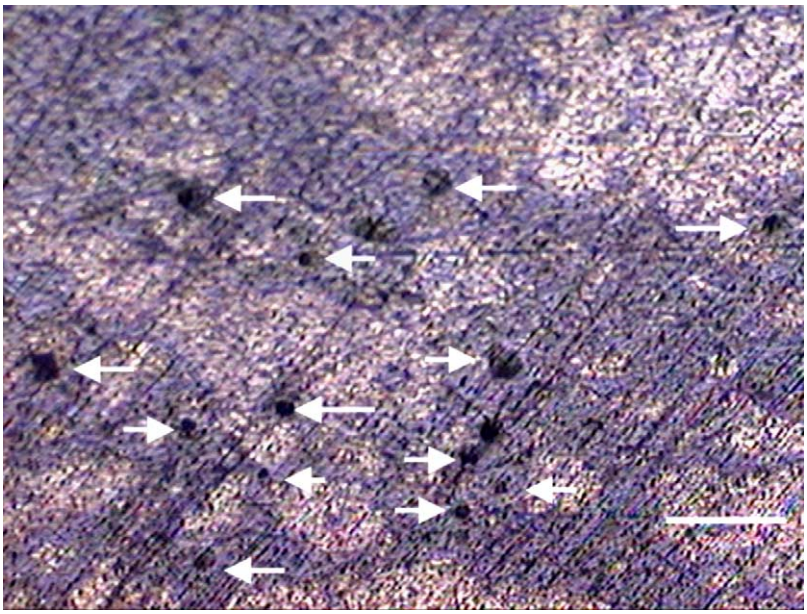

Fig. 5. Optical microphotograph of composite bipolar plate with 60 wt.% graphite content (×100).

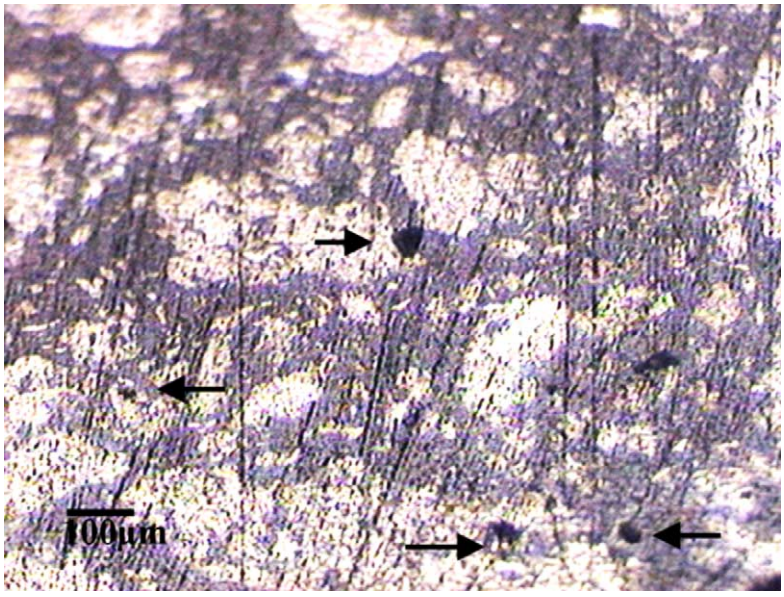

Fig. 6. Optical microphotograph of composite bipolar plate with 70 wt.% graphite content (×50).

decreased. Consequently, the electrical resistance of the composite bipolar plate decreases as the particle size of the graphite powder decreases.

3.5. Thermal properties

The TMA curves of vinyl ester resin are given in Fig. 13. The glass transition temperature is 182 °C. Since the working temperature of PEMFC is about 80–l00 °C, the composite bipolar plate is thermally stable over this range. The TGA curve of for the composite bipolar plate are presented in Fig. 14. The value of the temperature of degradation at which the weight loss of material is 5% (Td5) occurs at 268 °C. This also confirms the good thermal stability of the plate.

The thermal expansion of the composite bipolar plate decreases with increasing in graphite content from 37.33 μm/m °C (60 wt.%) to 8.55 μm/m °C (80 wt.%), see Fig. 15. The expansion decreases with decreasing graphite size from 16.85 μm/m °C (1000–l77 μm) to 8.89 μm/m °C (less than 53 μm). On increasing the temperature from 25 to 100 °C, the graphite powder will shrink, while the resin will expand. Hence, graphite will reduce the thermal expansion of the resin matrix during the heating process and, in turn, the expansion of the composite bipolar plate.

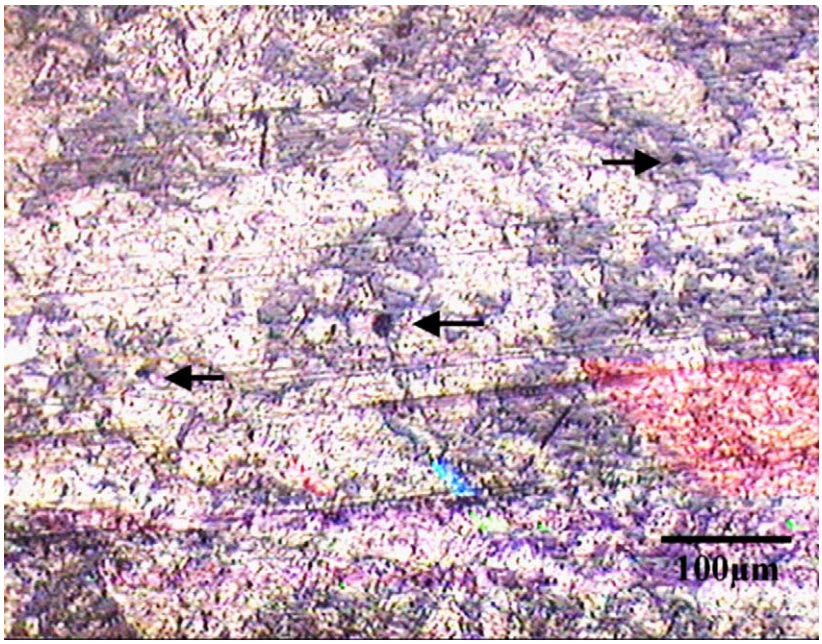

Fig. 7. Optical microphotograph of composite bipolar plate with 75 wt.% graphite content (×100).

Fig. 8. Optical microphotograph of composite bipolar plate with 80 wt.% graphite content (×50).

The number of voids in the composite bipolar plate increases as the graphite size decreases. Thus, expansion during the heating process will become insignificant. Consequently, thermal expansion of the composite bipolar plate decreases as the graphite size decreases.

3.6. Oxygen permeability

The oxygen permeability is least for a composite bipolar plate with 75 wt.% graphite ($5.82 \times 10^{-}8\,cm^3/cm^2\,s$). If increases with decreasing graphite size from 6.76×10^{-8} (1000–177 μm) to $3.28 \times 10^{-5}\,cm^3/cm^2\,s$ (less than 53 μm). This is because graphite has a planar structure that is capable of blocking the gas permeability.

3.7. Flexural property

The flexural strength of the composite bipolar plate decreases with increasing graphite content from 38.47 MPa (60 wt.%) to 27.3 MPa (80 wt.%), as shown in Fig. 19. The flexural modulus decreases with increasing graphite content from 9011 MPa (60 wt.%) to 6621 MPa (80 wt.%),

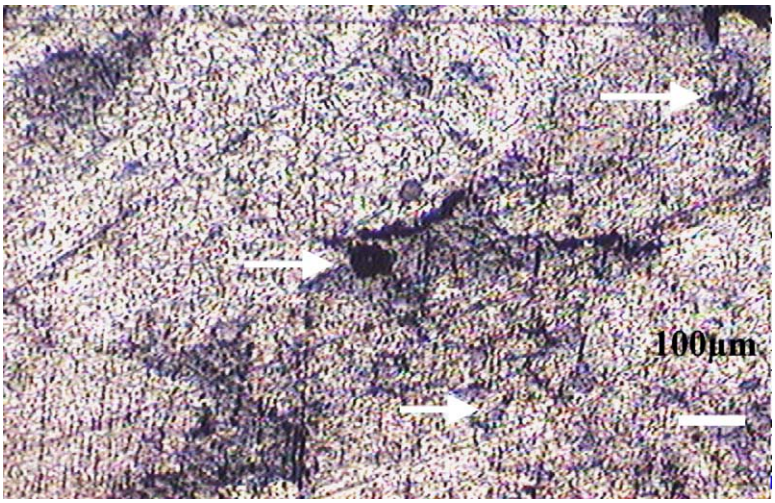

Fig. 9. Optical microphotograph of composite bipolar plate with 75 wt.% graphite content and with graphite powder diameter >77 μm (×50).

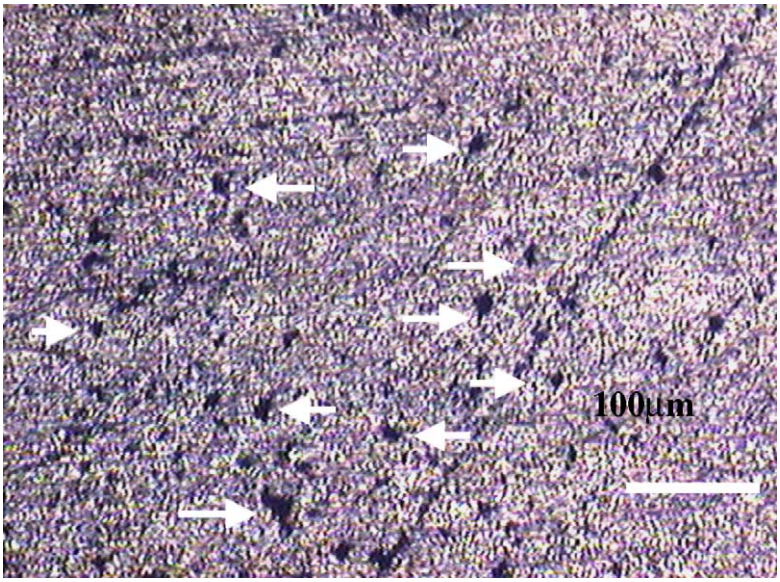

Fig. 10. Optical microphotograph of composite bipolar plate with 75 wt.% graphite content and with graphite powder diameter <53 μm (×100).

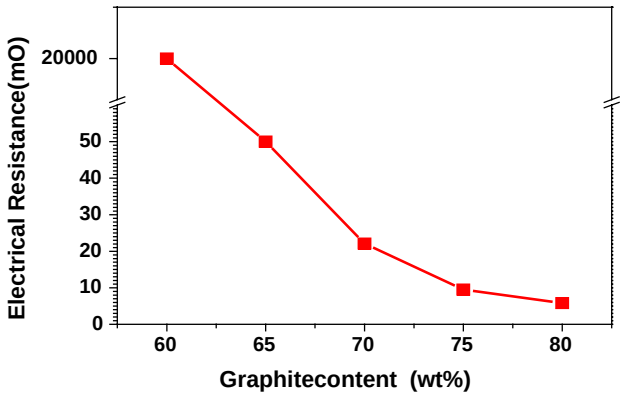

Fig. 11. Electrical resistance of composite bipolar plate with different graphite contents.

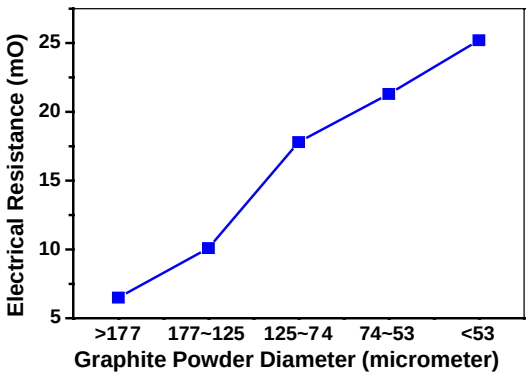

Fig. 12. Electrical resistance of composite bipolar plate with 75 wt.% graphite content and with different graphite powder sizes.

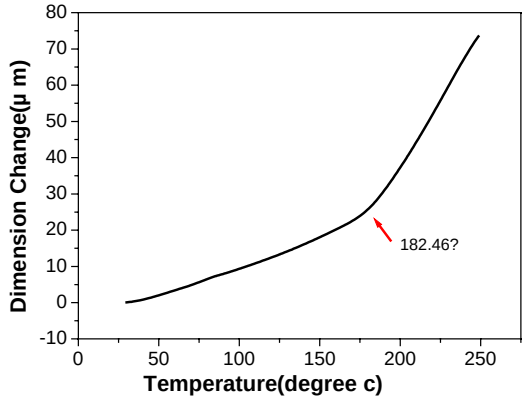

Fig. 13. TMA curves of vinyl ester resin.

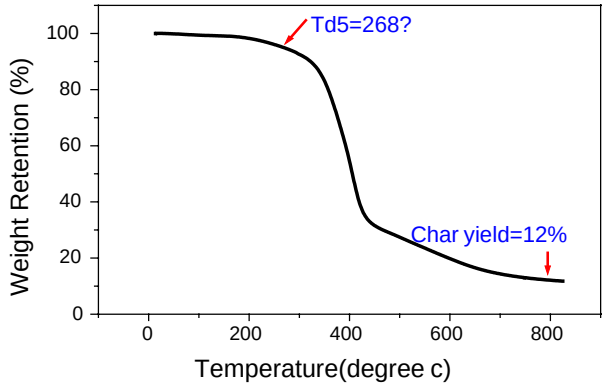

Fig. 14. TGA curves of vinyl ester resin.

see Fig. 20. The flexural strength decreases with decreasing graphite size from 31.23 MPa (1000–l77 μm) to 15.96 MPa (less than 53 μm). The flexural modulus of the composite bipolar plate decreases with decreasing graphite size from 6923 MPa (1000–177 μm) to 4585 MPa (less than 53 μm). The adhesion between resin and graphite become weaker as the graphite content increased. Consequently, the flexural property of the composite bipolar plate decreases as the graphite content increased. Small-size graphite powder possesses more surface area than longer graphite powder.

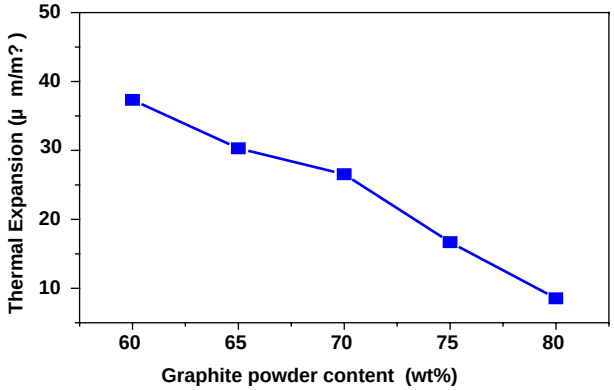

Fig. 15. Thermal expansion of composite bipolar plate with different graphite contents.

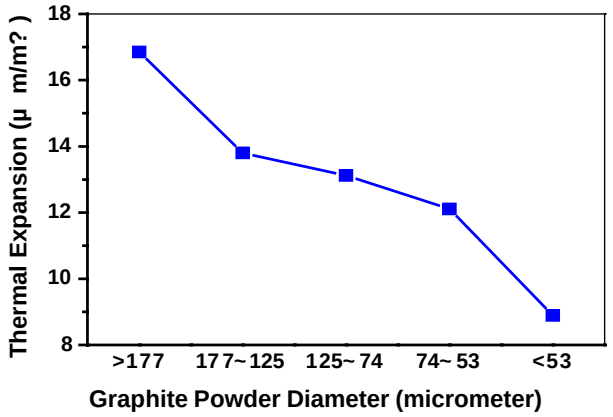

Fig. 16. Thermal expansion of composite bipolar plate with 75 wt.% graphite content and with different graphite powder sizes.

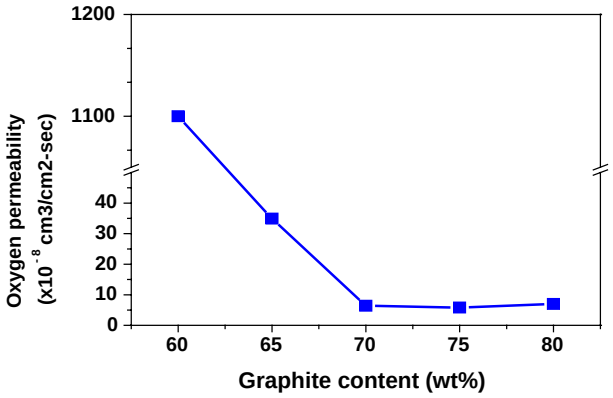

Fig. 17. Oxygen gas permeability of composite bipolar plate with different graphite contents.

Hence, small-size graphite powder with 75 wt.% graphite content has a stronger absorbing ability than that of longer graphite powder. The porosity and number of voids increases with decreasing graphite size. Hence, the flexural property of the composite bipolar plate decreases with decreasing graphite size, which is shown in Figs. 16–22.

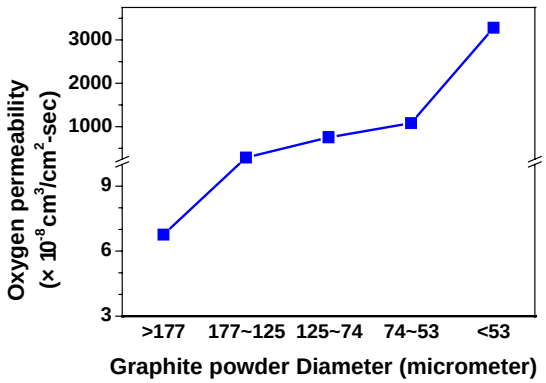

Fig. 18. Oxygen gas permeability of composite bipolar plate with 75 wt.% graphite content and with different graphite powder sizes.

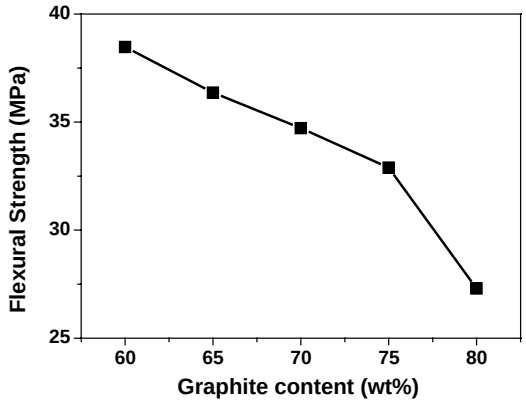

Fig. 19. Flexural strength of composite bipolar plate with different graphite contents.

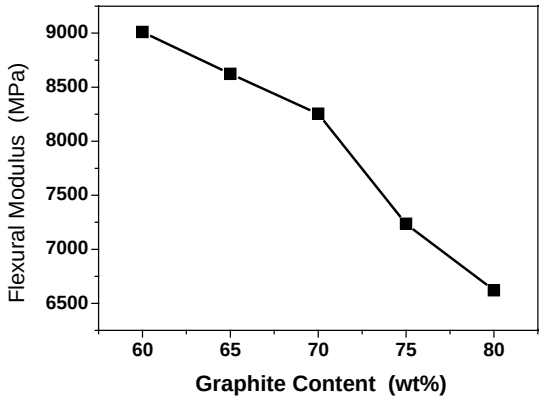

Fig. 20. Flexural modulus of composite bipolar plate with different graphite contents.

3.8. Corrosion property

The corrosion currents of composite bipolar plates with different graphite contents and graphite size are summarized in Tables 2 and 3.The difference in corrosion current between 60 and 80 wt.% graphite is small, see Fig. 23. the difference between 1000–177 and <53 μm graphite is small,

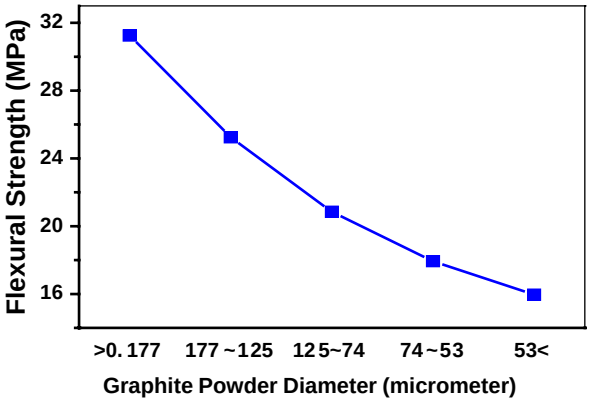

Fig. 21. Flexural strength of composite bipolar plate with 75 wt.% graphite content and with different graphite powder sizes.

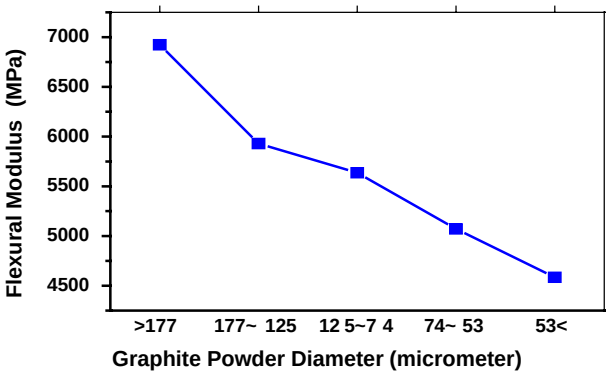

Fig. 22. Flexural modulus of composite bipolar plate with 75 wt.% graphite content and with different graphite powder sizes.

Table 2
Corrosion current of composite bipolar plate with different graphite contents

Graphite content (wt.%)	Corrosion current (A cm^{-2})
60	8.0×10^{-7}
65	7.5×10^{-7}
70	7.0×10^{-7}
75	3.6×10^{-7}
80	3.0×10^{-7}

Table 3
Corrosion current of composite bipolar plate with 75 wt.% graphite content and with different particle sizes

Graphite powder diameter (μm)	Corrosion current (A cm^{-2})
>177	1.8×10^{-9}
177–125	9.0×10^{-8}
125–74	8.0×10^{-8}
74–53	7.5×10^{-8}
>53	1.2×10^{-7}

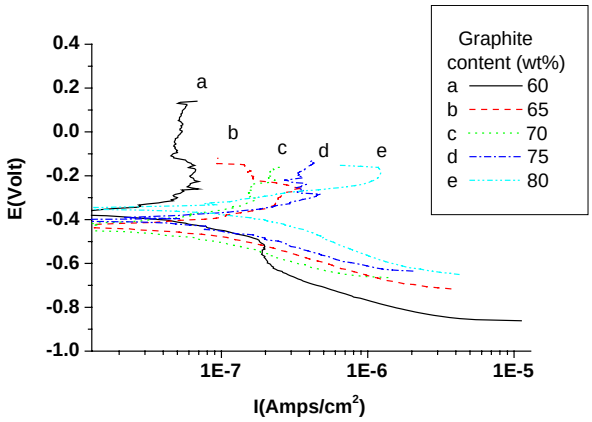

Fig. 23. Corrosion current of composite bipolar plate with different graphite contents.

see Fig. 24. The corrosion current is less than 10^{-7} A cm^{-2} when the graphite content is higher than 60 wt.%, i.e., the composite bipolar plate is fully corrosion-resistant under this condition.

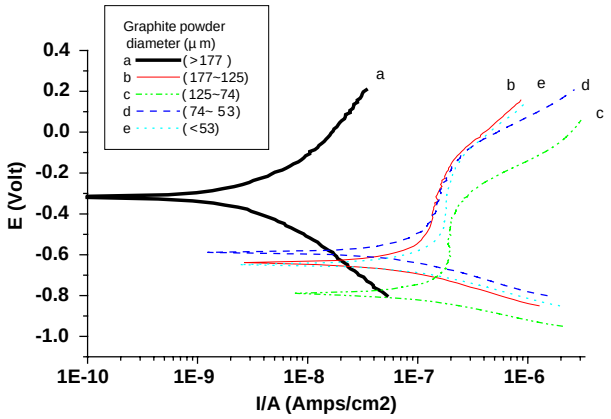

Fig. 24. Corrosion current of composite bipolar plate with 75 wt.% graphite content with different graphite powder sizes.

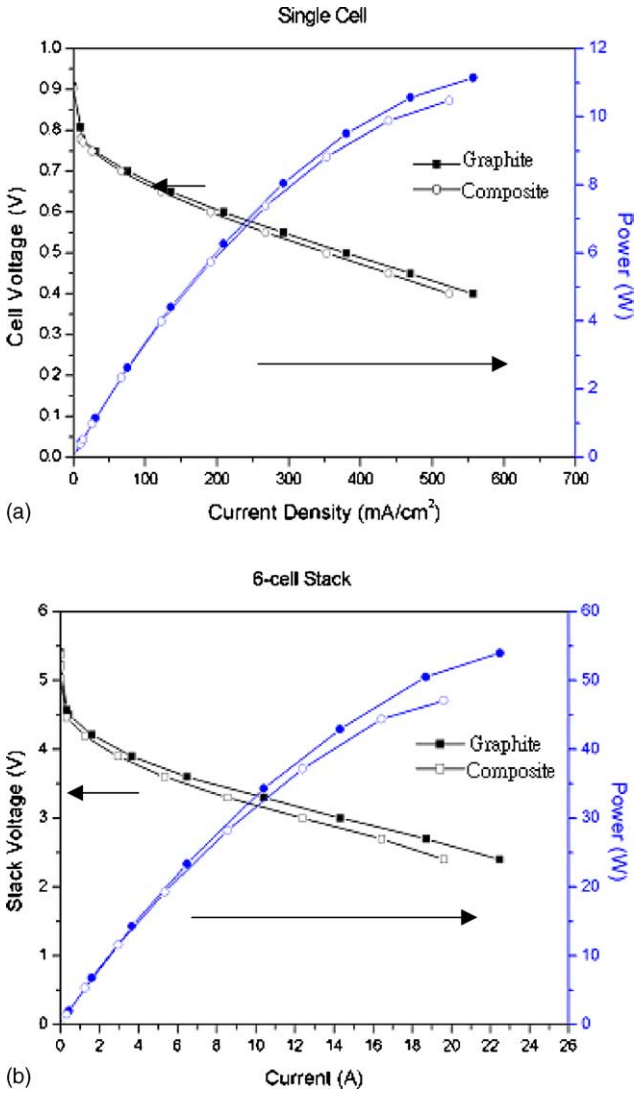

Fig. 25. (a) Comparison of *I–V* performance of graphite bipolar plate and composite bipolar plate (single cell test). (b) Comparison of *I–V* performance of graphite bipolar plate and composite bipolar plate (6-cell stack test).

Table 4
UL-94V-0 and LOI test results of vinyl ester/graphite composite systems with different graphite contents

Graphite content (wt.%)	Flaming drops	Cotton ignited	UL-94V-0 standard	LOI
60	N/A[a]	N/A	94V-0	>50
65	N/A	N/A	94V-0	>50
70	N/A	N/A	94V-0	>50
75	N/A	N/A	94V-0	>50
80	N/A	N/A	94V-0	>50

[a] Not available.

Table 5
The UL-94V-0 and LOI test results of vinyl ester/graphite composite systems with 75 wt.% graphite contents and with different graphite powder sizes

Graphite powder diameter (μm)	Flaming drops	Cotton ignited	UL-94V-0 standard	LOI
>177	N/A[a]	N/A	94V-0	>50
177–125	N/A	N/A	94V-0	>50
125–74	N/A	N/A	94V-0	>50
74–53	N/A	N/A	94V-0	>50
<53	N/A	N/A	94V-0	>50

[a] Not available.

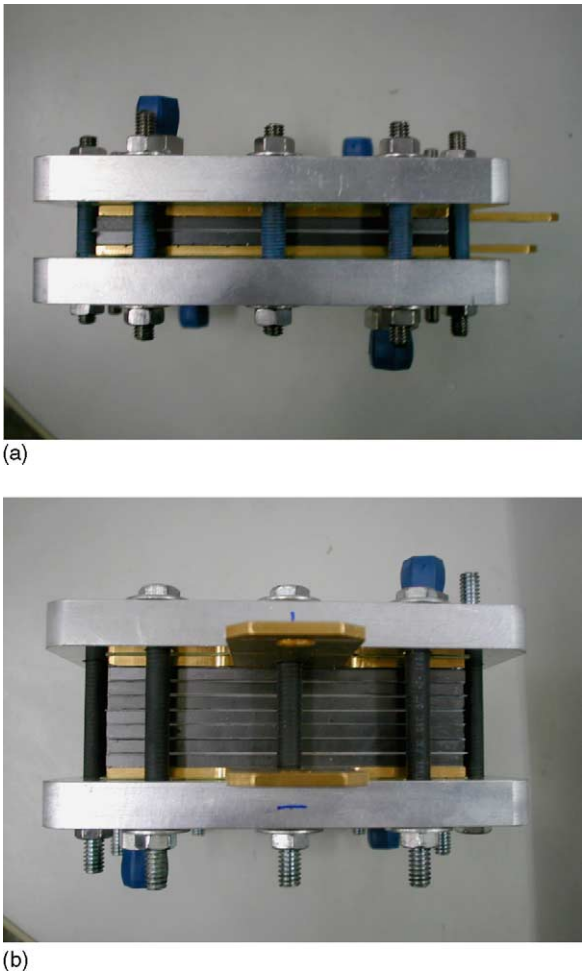

(a)

(b)

Fig. 26. Photographs of (a) single cell using the composite bipolar plate, (b) 6-cell stack using the composite bipolar plate.

3.9. Flame retardance

The flame resistance of the composite bipolar plate when graphite content is changed from 60 to 80 wt.% is shown in Table 4; corresponding data for a change in graphite size from 1000–177 to <53 μm are given in Table 5. The composite bipolar plate meets UL-94V-0 and LOI >50 specifications, possesses good flame retardance as when the graphite content is above 60 wt.%.

3.10. I–V Performance of single cell and 6-cell stack

The *I–V* and *I–P* performance of a composite bipolar plate and a graphite bipolar plate for single cell and 6-cell stack are given in Fig. 25(a) and (b), respectively. Photographs of the single cell and the 6-cell stack using the composite bipolar plate are presented in Figs. 26(a) and (b), respectively. The *I–V* performance of composite bipolar plate is very similar to that of the graphite bipolar plate, and so is the *I–P* performance. The data indicate that the optimum composition (75 wt.%) of the composite bipolar plate provides a suitable replacement for the graphite composite plate.

4. Conclusions

A composite bipolar plate composed of vinyl ester resin and graphite has been successfully prepared by the BMC process. The glass transition temperature of vinyl ester resin is 182 °C. The thermal stability of the composite bipolar plate is thermally stable above 250 °C.

The density of the composite bipolar plate increases from 1.49 to 1.82 as the graphite content is increased from 60 to 80 wt.%, and decreases from 1.70 to 1.45 as the graphite size decreases from 1000–177 to <53 μm. The porosity of composite bipolar plate increases from 0.06 to 2.64% as the graphite content is increased from 60 to 80 wt.%, decreases from 0.571 to 15.45% as the graphite size is decreased from 1000–177 to <53 μm. The number of voids in the composite bipolar plate is smallest when the graphite content is 75 wt.%. The number of voids increases as the graphite size is decreased from 1000–177 to <53 μm. The electrical resistance of composite bipolar plate decreases from 20 000 to 5.8 mΩ as the graphite content is increased from 60 to 80 wt.% and increases from 6.5 to 25.2 mΩ as the graphite size is decreased from 1000–177 to <53 μm. The thermal expansion of the composite bipolar plate decreases from 37.33 to 8.55 μm/m °C as the graphite content is increased from 60 to 80 wt.% and decreases from 16.85 to 8.89 μm/m °C as the graphite size is decreased from 1000–177 to <53 μm. The oxygen permeability of the composite bipolar plate is smallest when the graphite content is 75 wt.%. The oxygen permeability increases from 6.76×10^{-8} cm^3/cm^2 s (1000–177 μm) to 3.28×10^{-5} cm^3/cm^2 s (less than 53 μm). The flexural strength of composite bipolar plate decreases from 38.47 MPa (60 wt.%) to 27.3 MPa (80 wt.%) as the graphite content is increased. The flexural modulus of the composite bipolar plate decreases from 9011 MPa (60 wt.%) to 6621 MPa (80 wt.%) as the graphite content is increased. The corrosion currents for the composite bipolar plate containing different graphite content and graphite size are all less than 10^{-7} A cm^{-2}. Composite bipolar plates containing different graphite contents and graphite sizes meet UL-94V-0 specification and the LOI are higher than 50. From electrical resistance and oxygen permeability studies, the composite bipolar plate with 75 wt.% graphite with a size between 1000 and 177 μm, shows optimum properties. The composite bipolar plate also shows excellent flame retardance (meets UL-94V-0 and LOI >50) and good corrosion resistance (less than 10^{-7} A cm^{-2}). Both *I–V* and *I–P* tests show that composite bipolar plates with optimum composition possess equivalent performance to a graphite bipolar plate.

Acknowledgements

The authors are grateful to the Ministry of Economics Affairs for financial support. Assistance with cell testing by Enliang Enterprise Co., Ltd., Taiwan is also great appreciated.

References

[1] J. Larminie, A. Dicks, Fuel Cell Systems Explained, Wiley, 2001.
[2] R.C. Makkus, A.H.H. Janssen, F.A. de Bruijn, R.K.A.M. Mallant, Fuel Cells Bull. 3 (17) (2000) 5–9.
[3] M.S. Wilson, Composite bipolar plate for electrochemical cells, WO00/25372, 2000.
[4] M.K. Bisaria, Injection moldable conductive aromatic thermoplastic liquid crystalline polymer compositions, WO00/44005, 2000.
[5] J. Wind, R. Spah, W. Kaiser, G. Bohm, J. Power Sources 105 (2002) 154–158.
[6] D.P. Davies, P.L. Adcock, M. Turpin, S.J. Rowen, J. Power Sources 86 (2002) 237–242.
[7] R.C. Makkus, A.H.H. Janssen, F.A. de Bruijn, R.K.A.M. Mallant, J. Non-Cryst. Solids 173 (1–3) (1985) 681.
[8] R. Hornung, G. Kappelt, J. Power Sources 72 (1998) 20–21.
[9] http://www.plastictechnology.com, website, 2002.
[10] http://www.h2economy.com, website, 2002.